POAC'15
Trondheim, Norway

Proceedings of the 23rd International Conference on
Port and Ocean Engineering under Arctic Conditions
June 14-18, 2015
Trondheim, Norway

AN ENGINEERING APPROACH TO STUDY THE TOWING OF A FOUR-LEG GBS IN SEA ICE

Wenjun Lu[1,2], Dagfinn Hagen[2], Hilde Benedikte Østlund[2]
[1)]*SAMCoT, NTNU, Trondheim, Norway*
[2)] *Kvaerner Concrete Solution AS, Oslo, Norway*

ABSTRACT

Towing a large volume Gravity Based Structure (GBS) in ice-covered waters is rather challenging. According to previous experiences, ice management should be considered as an indispensable component of such a demanding operation. In addition, a good towing configuration (i.e., number of towing vessels and towing spread) can also maximise the efficiency. As an initial phase study, under the assumption of a reasonably managed ice condition, this paper focuses on the theoretical study to resolve different conflicting factors (i.e., ice resistance, towing distance and towed vessels' arrangement) while designing a reasonable towing configuration in ice covered waters. Specifically, the upper-bound ice resistance was calculated to estimate the required number of towing vessels. Based on the calculation, a conservative estimation suggests that 5 towing vessels with a bollard pull of 200 ton each is necessary to tow the considered GBS in pressurised ice conditions. Then a lower-bound ice resistance model was developed based on previous available models. This lower bound is utilised to calculate a safe distance between the towing vessel and towed structure. Calculations show that a braking mechanism can effectively reduce the safe distance. In order to optimise the towing spread, the propeller wash effect was further investigated. Variables such as towing distance, lateral location of the towing vessels and propeller diameters were studied with existing models. It is found that the side vessel is better to be located a distance of 80 m away from central line, such that the ice clearing effect can be maximised and in the meantime collision risk is reduced. Based on all these models' calculation results, an initial towing configuration is proposed at the end of this paper. Future studies to include 'optimised ice management strategies' and 'more information on ice conditions' can be directly built upon models and numerical scripts developed in this paper.

1. INTRODUCTION

Comparing to the well-established towing operation in open water (Nielsen, 2007; Veritas, 2011), towing an offshore structure in sea ice poses additional challenges. The varieties of sea ice features (e.g., level ice, ice ridges, pack ice etc.) and its varying drifting pattern complicate the design and execution of the towing operation. All these complications root essentially in the potentially large and directional varying ice load. In order to alleviate the ice load to an acceptable level, an effective Ice Management (IM) is considered essential (Wright, 1999). Therefore, two interconnected systems, i.e., the towing configuration and the associated IM strategy, should be designed and optimised in an iterative manner.

Ice Management (IM) operations have been performed in many different projects (e.g., a review work is presented by Eik (2008). In addition, several IM trials were carried out for study purpose (e.g., (Farid et al., 2014; Hamilton et al., 2011; Maddock et al., 2011; Scibilia et al., 2014)). However, the afore mentioned IM operations were mainly designed to protect a stationary object. IM for a towing operation differs due to the mobility of the towed structure and also the transit speed requirement imposed to the operation. The designs of the towing operation (e.g., the towing configuration) are interconnected with the associated IM strategy.

Towing configuration considerations include the amount of towing tugs and their geometric deployment (i.e., the tow spread). This demands a knowledge on the ice load level on the towed structure. Available field measurements for similar structures can serve as a good reference for the expected load level. However, a marked difference exists in the consideration of ice load on a towed structure and other 'stationary' moored/fixed structures, i.e., we need to think about the interaction between the towed structure and towing vessels. This paper studies the towing configuration under a 'reasonable' IM operation. Conflicting factors such as towing distance favourable for directional control, no collision safe distance between the towed structure and towing vessels, and propeller wash effect are theoretically studied. The offshore structure under this study is chosen as a large concrete GBS with self-floating capability. Moreover, former experiences (i.e., towing operation of Kulluk) were extensively utilised for comparison.

2. HISTORICAL TOWING OPERATIONS

In history, several offshore structures have been towed in ice, e.g., the Kulluk (Hnatiuk and Wright, 1984; Loh et al., 1984), the Single Steel Drilling Caisson (SSDC) (Walsh et al., 1994) and Molikpaq (Gijzel et al., 1985). Their successful experiences contribute greatly to the studies made in this paper.

2.1 Towing operation of Kulluk

For the successful towing operation of Kulluk in ice (see Figure 1), 'occasional' ice management has been carried out by three supporting icebreakers. In addition, it was shown that deploying two icebreakers separately at the one quarter shoulder of Kulluk facilitated the rubble transportation process and thus alleviated the load level (Hnatiuk and Wright, 1984; Loh et al., 1984). Only one icebreaking vessel, Kalvik, was carrying out the towing operation while the other three supporting icebreaking vessels are either breaking the incoming ice, widening the channel or strengthening the rubble flow around Kulluk via propeller wash. This configuration was termed as the 'best' strategy by Hnatiuk and Wright (1984) and it leads to a transit speed of several knots in 30 - 60 cm thick level ice conditions.

Among all the valuable experiences, the following two points are highlighted while designing the towing configuration:

- Propeller wash to facilitate the rubble transportation was demonstrated effective;
- A short towing line is utilised to achieve directional control though it is susceptible to high impulse loading (Browne et al., 1984).

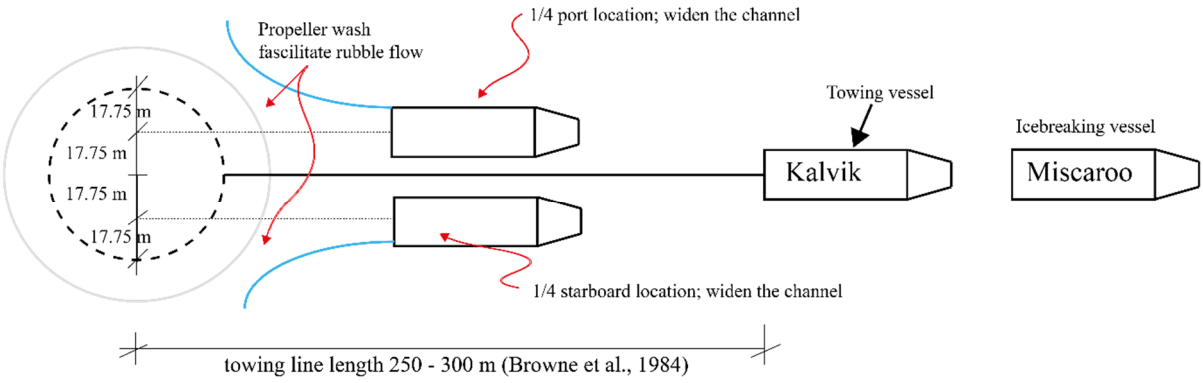

Figure 1. Conceptual plot of the towing operation according to the descriptions of Hnatiuk and Wright (1984).

2.2 Towing operation of the Single Steel Drilling Caisson (SSDC)

Based on experiences obtained from six successfully relocations, three ice-class[1] vessels were considered optimal in towing the SSDC in ice (Walsh et al., 1994). Depending on the environment, the tow spread is illustrated in Figure 2 while towing in ice.

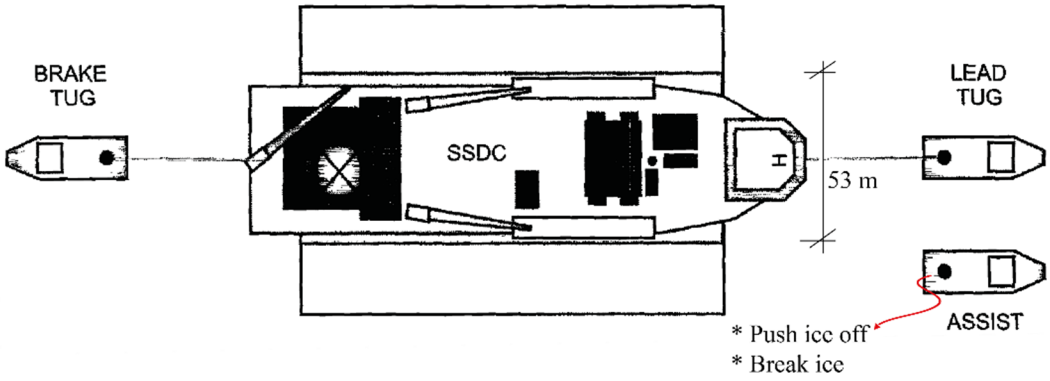

Figure 2. Towing configuration of the SSDC (from Walsh et al. (1994)).

From this operation, a brake tug was utilised. Though this was not explicitly explained, it is thought to be a precaution against overrun against towing vessels due to a short towing line. It was reported by Wright (1998) that the longest towing lines in lower ice concentration is only about 150 m.

Based on the previous experiences, we raise the following questions for the towing operation of a GBS in sea ice:

1) How many towing vessels are needed?
2) What towing configuration can optimise the following conflicting factors?
    a) Short towing distance for directional control;
    b) Short towing distance for propeller wash of ice rubbles;
    c) Long towing distance to avoid potential collision.

From a theoretical point of view, the above questions are addressed with existing theories. In order to estimate the amount of towing vessels, an upper-bound ice resistance of the considered structure is estimated in Section 4.1. For the collision time estimation, a lower-bound resistance is estimated in Section 4.2. The propeller wash effect was studied by integrating the propeller momentum according to different towing configuration in Section 5.

[1] Initially, five vessels were utilised.

3. THE GRAVITY BASED STRUCTURE

This paper focuses on the towing operation study of a large self-floating Gravity Based Structure (GBS). All the methodologies presented are directly applied to this particular structure with reference to other structures. Figure 3 illustrates its underwater geometry. During most of the towing journey, the large box-shaped pontoon is submerged such that only four identical cylindrical legs pierce out of the water plane. This can largely minimise the contact areas with the drifting sea ice, thereby reducing the overall ice load. Based on the displaced water volume, the overall mass of the GBS is about 341,000 tons, which is about 10 times of that of Kulluk (32,500 tons) (Browne et al., 1984). This indicates that significant bollard pull from tugs and a long duration are required to accelerate/decelerate the GBS to required towing speed.

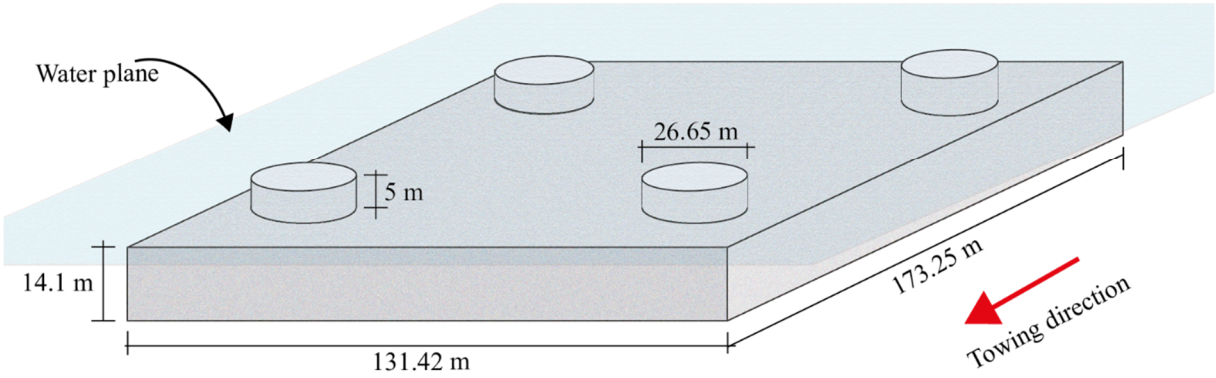

Figure 3. The underwater geometry of the studied self-floating GBS.

The towing resistance consists of two parts, i.e., fluid resistance and ice load. In this study, we study them separately in a decoupled manner. For now, we do not pay special attention to the Marginal Ice Zone (MIZ). The wave drifting force (Faltinsen, 1993) is thus neglected. Only the drag force F_d due to the relative velocity between the towed structure and ambient fluid is considered and is expressed in Eq. (1).

$$F_d = \frac{1}{2} C_d \rho_w A V |V| \tag{1}$$

in which,

- C_d drag coefficient. Detailed values for the components of GBS are listed in Table 1 according to recommendations set forth by Det Norske Veritas (2011);
- ρ_w water density and it is treated as a constant 1025 $\mathrm{kg/m^3}$ throughout the study;
- A underwater part of the towed structure's projected area normal to the towing direction;
- V average velocity (i.e., vector) of the GBS relative to the ambient fluid.

Table 1. Drag force of the GBS.

	C_d	$A\,[\mathrm{m^2}]$	$F_d(V=1\,\mathrm{m/s})$ [ton]	$F_d(V=1.5\,\mathrm{m/s})$ [ton]	$F_d(V=2\,\mathrm{m/s})$ [ton]	$F_d(V=3\,\mathrm{m/s})$ [ton]
Cylinder	0.8	113.25	5	10	19	42
Pontoon	2	2510.1	257	579	1029	2316
Total		2963.1	276	621	1103	2483

Eq. (1) is applied to the towed structure in Figure 3 and the results under different towing speed is presented in Table 1. It shows that two tugs with a bollard pull of 200 ton each are required

to maintain a speed of 2 knot (1 m/s) even in calm water (no wave). This drag force is highly velocity dependent and shall be utilised to estimate a no collision safe distance between the towing vessels and the towed structure in Section 4.2.

4. ICE RESISTANCE ESTIMATION

Apart from the water resistance, a good estimation of the potentially encountered ice resistance is another prerequisite in designing the towing configuration (e.g., number of the towing tugs). However, managed ice resistance calculation is rather complicated. It involves fracture of finite sized ice floe (Lu, 2014; Lu et al., 2015a; Lu et al., 2015b; Lu et al., 2015c), more research aspects in hydrodynamic considerations (Tsarau et al., 2015; Tsarau et al., 2014), and multi-body dynamics to account for rubble accumulation and transportation (Lubbad and Løset, 2011; Metrikin and Løset, 2013). More parameters, e.g., floe size, ice concentration and ice pressure are required to describe a managed ice field. For the current paper, we do not go into detailed numerical analysis to calculate the corresponding managed ice resistance. Instead, we adopt and derive straightforward analytical solutions to make an upper and lower-bound estimation of what we believe is the potential managed ice resistance.

4.1 Upper-bound ice resistance and towing vessels numbers

Wright (1999) documented the measurement of managed ice resistance experienced by Kulluk. The author grouped the data into scenarios with good clearance (i.e., 'slurry' flow around Kulluk) and those under ice pressure (i.e., formation of rubble wedge). Based on the upper bound of Wright's (1999) measurement, Croasdale et al. (2009) proposed an analytical model (see Eq. (2)) to calculate managed ice resistance in a pressurised ice field.

$$F_{pressure\_ice} = pDt(1+\frac{\mu_i}{\tan\alpha})+\frac{cDt}{\tan\alpha} \quad (2)$$

in which,

- $F_{pressure\_ice}$ resistance due to a pressurised managed ice field;
- p pressure built up within the managed ice field. It is relevant to the wind speed, wind fetch length on ice, and potential ridge building (Palmer and Croasdale, 2013);
- D size of the baseline length of the rubble wedge, e.g., $D = 26.65\,\text{m}$ and $D \approx 131.42\,\text{m}$ in Figure 4a and b respectively;
- t ice thickness. In all calculations, we choose $t = 1.2\,\text{m}$ representing what could be first-year ice conditions;
- μ_i ice-ice friction;
- α half the angle of the rubble wedge (see Figure 4);
- c background cohesion introduced by Croasdale et al. (2009).

According to Croasdale et al. (2009), it is found that $p = 15\,\text{kPa}$, $\mu_i = 0.1$, and $c = 2\,\text{kPa}$ can best fit the upper bound of measured data from Kulluk under pressurised ice conditions. In this regard, we utilised these fitted inputs together with Eq. (2) to potential rubble wedge formations scenarios upon the GBS. Two conservative scenarios are illustrated in Figure 4, i.e., rubble wedge formation in front of four cylinder legs (Figure 4a) and rubble wedge formation upon a rubble arch which bridges the two front legs of the GBS (Figure 4b).

After inserting the baseline length D for the above two different scenarios, the results are presented in Table 2. The calculations are based on two different ice pressure values $p = 15\,\text{kPa}$ and $p = 30\,\text{kPa}$. According to Croasdale et al.'s (1988) measurement in Beaufort sea, in most cases, the ice pressure is negligible. Only when the ice thickness reaches maxima in April and under a strong towards shore wind, was a pressure range between 19~29 kPa observed.

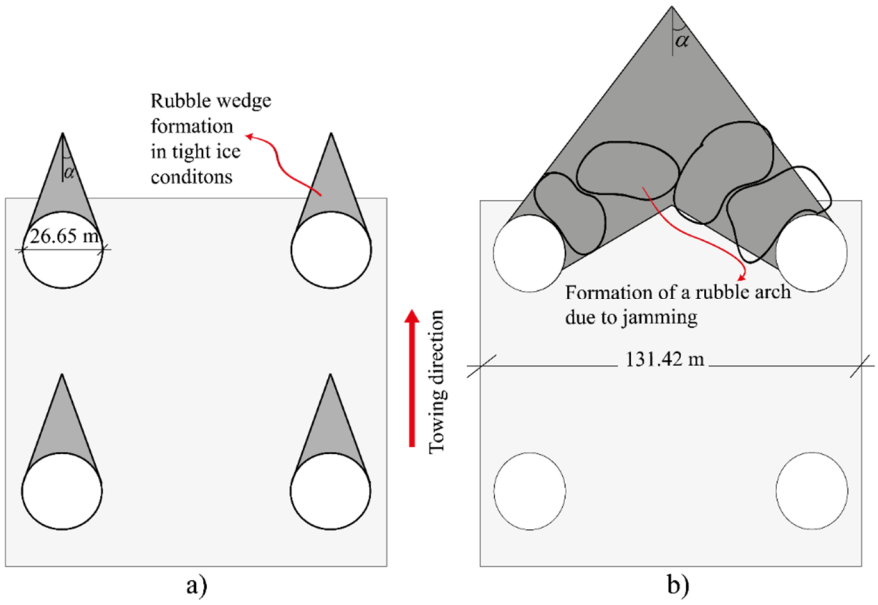

Figure 4. Rubble wedge formation scenarios in front of the GBS legs.

As indicated by Table 2, the results are rather sensitive to the level of ice pressure, which has a higher uncertainty than the ice thickness. However, we should bear in mind that the calculation of Eq. (2) is more for a stationary structure, whereas in a towing operation, the constant movement of the structure reduces the chances of such rubble wedge formation. For instance, while Kulluk was staying in position, as high as 236 tons (see Table 2) resistance were detected. However, during its towing operation in rather heavy pack ice conditions, a towing line tension of about 150 tons is sufficient to sustain a transit speed of 3 knots (Wright, 1998). This corresponds to an ice resistance of about 230 tons for the GBS when a linear extrapolation was adopted.

Table 2. Managed ice resistance assuming ice wedge formation (i.e., tight ice condition).

	p [kPa]	D [m]	t [m]	$F_{pressure\_ice}$ [ton]
GBS scenario 1	30	26.65×4	1.2	623
GBS scenario 2	30	130	1.2	759
GBS scenario 1	15	26.65×4	1.2	**359**
GBS scenario 2	15	130	1.2	438
Kulluk (stationary)	15	70	1.2	236

Based on the above reasoning, as a conservative estimation of total ice resistance during towing operation, it seems sufficient to choose $p = 15$ kPa instead of $p = 30$ kPa to make an upper bound estimation on the potentially encountered ice resistance upon the GBS. However, the calculations made in Table 2 do suggest that:

- Sufficiently small ice floes should be produced by an IM operation to avoid jamming as in Scenario 2 (Figure 4b);
- A relatively open channel (less ice concentration) should be created to avoid any pressure built up as in Scenario 1 (Figure 4a).

Without pressure built up and with smaller floe sizes, the encountered ice resistance can be largely reduced. Nevertheless, with the resistance calculation in Tables 1 and 2, it is at our disposal to conservatively estimate the amount of towing vessels. Suppose that the towing

vessels (e.g., Kalvik, Tor Viking etc.) with a bollard pull in the order of 200 ton and 50 ton thruster is required for transiting in ice. This provides a net towing force of 150 ton. Adding up the resistance of the GBS from Tables 1 and 2, the required towing force and towing vessels are listed in Table 3. In addition, the experiences from Kulluk and SSDC are also appended in Table 3.

Table 3. A comparison of the required number of towing vessels.

	ice condition	Mass [ton]	waterline size [m]	Number of towing vessels (estimated towing capacity [ton])	Total resistance [ton] (and tow speed [m/s])
GBS_calculation	$p = 15\,\text{kPa}$	341 000	26.65×4	5 (750)	359+276=635 (1 m/s)
GBS_estimation	Linear extrapolation	341 000	26.65×4	4 (600)	230+276=506 (1 m/s)
SSDC (towing)[2]	Prebroken ice	90 000	Length: 162 width: 53	1	<200
Kulluk (towing)[3]	Heavy pack ice	32 500	71	1	150

4.2 Lower-bound ice resistance and collision time

During a towing operation, there is a possibility that towing vessels beset in ice or lose power due to mechanical/electrical failures. Therefore, it is necessary to set up a no collision safe distance between the towing vessel and the towed structure, particularly when the towed structure has a large mass.

In order to estimate the collision time, we need to estimate a lower bound of the ice resistance. From a physical point of view, when a free-floating structure enters a broken ice field, its initial kinetic energy is reduced by three major dissipative mechanisms. These are: 1) accelerating the neighbouring ice floes (increasing the kinetic energy of surrounding ice floes); 2) dissipation due to fluid drag force on the structure and neighbouring ice floes; and 3) contact dissipation among ice floes (e.g., crushing, shearing, and fracture due to floe contacts). In a highly concentrated ice field, it is mainly the third dissipation mechanism that is taking place (e.g., Eq. (2)). On the other hand, the first two mechanisms are dominate in a low concentration area (Marchenko et al., 2010). In order to estimate a lower bound for ice resistance, we neglect the third dissipation mechanism relating to material failure and also the shear drag force upon neighbouring ice floes.

In Appendix A, an influencing radius $R_{\text{influence}}$ is derived as in Eq. (3) (also see Figure 5) to describe the amount of neighbouring ice floes that have been displaced by the structure. This influencing radius is sensitive to the ice concentration c (e.g., $\lim_{Ic\to 0} R_{\text{influence}} = 0$ and $\lim_{Ic\to 1} R_{\text{influence}} = \infty$).

$$R_{\text{influence}} = \frac{\sqrt{Ic}}{1-\sqrt{Ic}}\frac{D}{2} \tag{3}$$

in which,

Ic represents the ice concentration.

Assuming that ice floes within the influencing zone obtain the same velocity as the structure after the interaction, we derived the following Eq. (4) to account for the average resistance in a loose ice field (see Appendix A).

[2] Data are mainly from Walsh et al. (1994);
[3] Data are mainly from Wright (1998).

$$F_{loose\_ice\_1} = \frac{Mm(2M+m)}{(M+m)^2}\frac{V^2}{D}$$
$$M = M_{GBS}(1+C_{am}) \quad (4)$$
$$m = \frac{\pi}{4}\left(\frac{\sqrt{Ic}}{1-\sqrt{Ic}}\right)\left(1+\frac{1}{2}\frac{\sqrt{Ic}}{1-\sqrt{Ic}}\right)\rho_i t D^2$$

in which,

$F_{loose\_ice\_1}$ resistance due to accelerating neighbouring ice floes within the influencing zone;

M_{GBS} mass of the considered GBS;

C_{am} added mass coefficient of the considered GBS and is conservatively estimated to be $C_{am} = 1$;

M overall mass effect from the GBS;

m generalised mass effect from the neighbouring ice floes in the influencing zone;

ρ_i density of sea ice and is assumed as $\rho_i = 920\ \mathrm{kg/m^3}$ in all calculations in this paper;

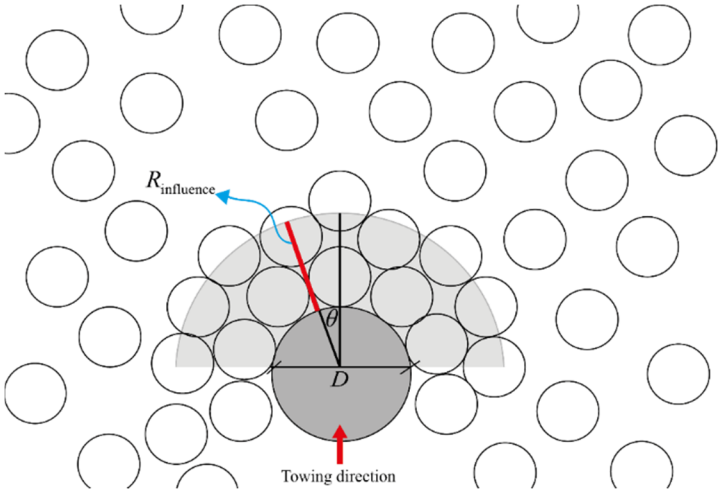

Figure 5. Illustration of the influencing radius in a loose broken ice field.

Eq. (4) is highly dependent on the ice concentration Ic. When a certain threshold of Ic_{cr} is exceeded, the resistance calculated by Eq. (4) becomes rather large. At this point, the footing failure formula (see Eq. (5)) proposed by Croasdale et al. (2009) is utilised to further lower the lower bound in loose ice conditions.

$$F_{loose\_ice\_2} = KcDt \quad (5)$$

in which,

$F_{loose\_ice\_2}$ is the resistance of a loose ice field and the ice rubble fails in a footing failure manner (Croasdale et al., 2009);

K reflects the slip plane length over the structural width and it is taken as 6 according to Croasdale et al.'s (2009) recommendation;

c is the background cohesion and was conservatively chosen as $c = 1\,\mathrm{kPa}$ according to Croasdale et al.'s (2009) fitting to Kulluk's measurement.

Using typical inputs introduced previously (i.e., $D = 26.65 \times 2$, $t = 1.2$, and $M_{GBS} = 341\,000\ \mathrm{ton}$), the results of Eqs. (4) and (5) are plotted in Figure 6. At low ice concentration, Eq. (4) predicts rather negligible ice resistance, which however, increases rapidly with increasing ice concentration. After crossing a threshold value calculated by Eq. (5), footing failure is expected

to be dominant and $F_{loose\_ice\_2}$ becomes the new lower bound of ice resistance. Collectively, we can write that the lower-bound ice resistance in loose ice condition can be expressed in Eq. (6).

$$F_{loose\_ice} = \min(F_{loose\_ice\_1}, F_{loose\_ice\_2}) \tag{6}$$

With the knowledge of a lower-bound resistance in different ice concentrations, we are able to calculate a no collision safe distance between the towing vessel and towed structure. Imagining that the towed structure is free floating in ice with a velocity of $V(\tau)$ at time τ, we can write the total resistance as in Eq. (7).

$$F_{resis\_L}(V^2(\tau)) = F_{loose\_ice} + F_d(V^2(\tau)) \tag{7}$$

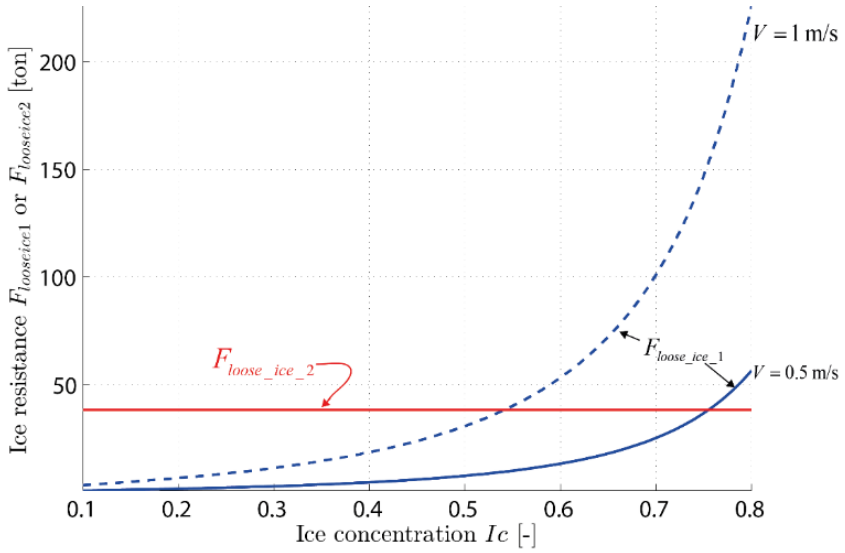

Figure 6. Lower-bound ice resistance in loose ice conditions.

Therefore, we can write the instantaneous acceleration $a(\tau)$, velocity $V(\tau)$ and travelling distance $S(\tau)$ in Eqs. (8), (9) and (10).

$$a(\tau) = -\frac{F_{resis\_L}(V^2(\tau))}{M} \tag{8}$$

$$V(\tau) = V(0) + \int_0^\tau a(s)ds = V(0) - \int_0^\tau \frac{F_{resis\_L}(V^2(s))}{M}ds \tag{9}$$

$$S(\tau) = \int_0^\tau V(x)dx = V(0)\tau - \int_0^\tau \int_0^x \frac{F_{resis\_L}(V^2(s))}{M}dsdx \tag{10}$$

The above integral equations can easily be solved with numerical methods. The numerical algorithm has been implemented in a MATLAB script and the results are presented in Figure 7 for the GBS with an initial speed of $V_0 = 1\,\text{m/s}$. Figure 7 demonstrates that with an increasing ice concentration, the GBS travels a shorter distance to reach certain speed limit. For example, if we define a velocity $V(\tau) = 0.1\,\text{m/s}$ as a safe velocity for handling collision, the no collision safe distance between towed structure and a towing vessel for various initial towing speed in various ice conditions are illustrated in Figure 8.

However, in reality, it is hard to define such a 'safe' speed limit. Should it be 0.1 m/s or 0.05 m/s? In addition, the theoretical calculation in Figure 7 shows that the towed structure would travel asymptotically to zero speed, i.e., they will never stop in calm water. Figure 8 also shows that the towing distance is too long in comparison to previous experiences (e.g., recalling that Wright (1998) documented a towing line length of 150 m in lower ice concentrations).

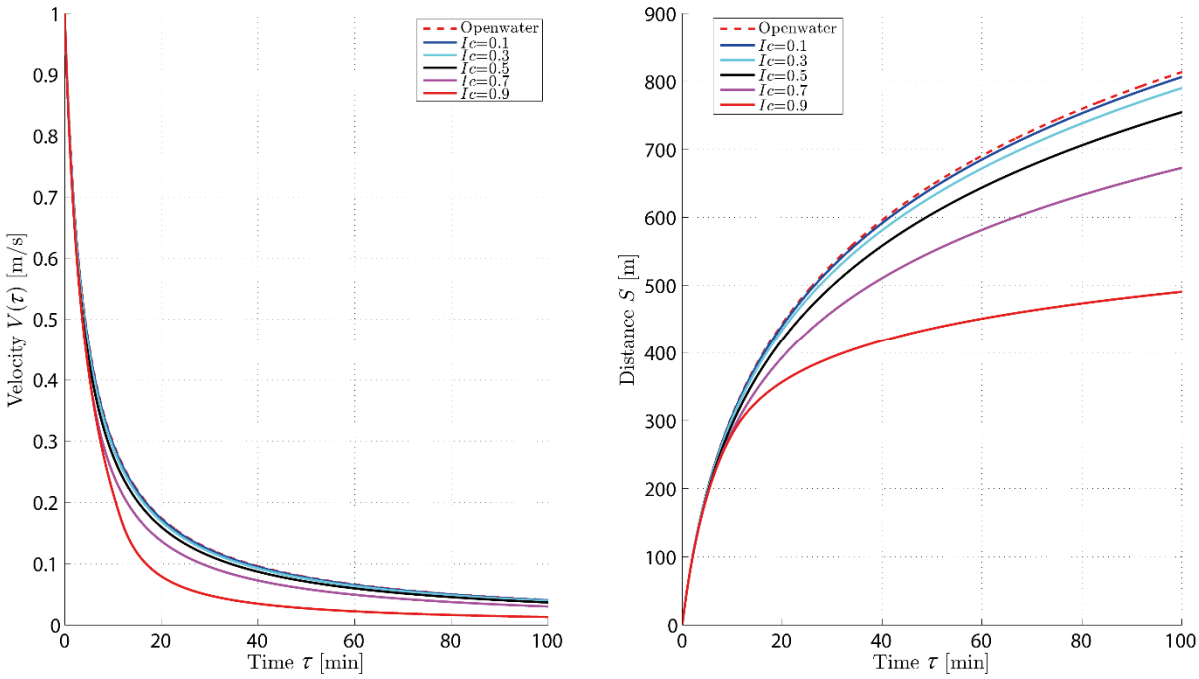

Figure 7. Velocity and displacement variation of the free-floating GBS with initial velocity of $V_0 = 1\,\text{m/s}$.

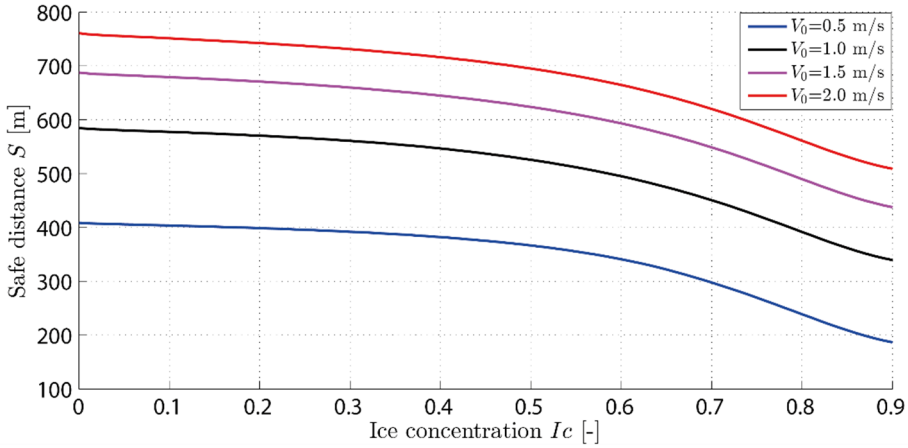

Figure 8. No collision safe distance between a free-floating towed structure and towing vessels in various ice conditions with different initial velocities (a threshold velocity of 0.1 m/s is used to calculate the travelling distance).

In order to shorten the towing distance (no collision safe distance) and also to make sure the towed structure is fully stopped, additional vessels can be used to brake the towed structure when necessary (e.g., see Figure 2). Suppose that it takes 10 min reaction time to have the braking vessel's effect on the towed structure, the velocity reduction and no collision safe distance for the same scenario in Figure 7 is recalculated in Figure 9 with a braking bollard pull of 200 ton. Figure 9 demonstrates that a braking system (e.g., braking vessels) can reduce the velocity to zero in less than 2 min and it can also effectively reduce the no collision safe distance. In lieu of this, we further investigated the influence of braking bollard pull and initial velocity on the no collision safe distance. The results are plotted in Figure 10. It shows that higher bollard pull leads to shorter no collision safe distance. However, the initial velocity is more influential in determining the no collision safe distance. Nevertheless, a comparison between Figures 8 and 10 demonstrates that a braking mechanism can largely reduce the required no collision safe distance.

Shorter towing distance means better propeller wash effect and turning capability, which are introduced in the next sections.

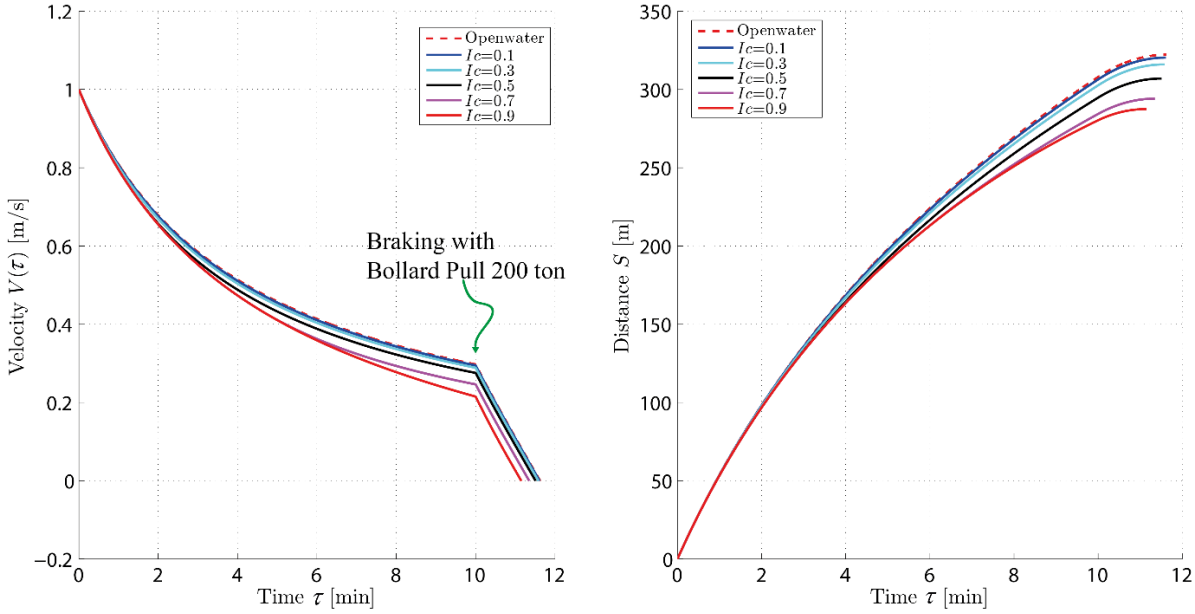

Figure 9. Velocity and displacement variation of the GBS with a 200 ton bollard pull braking vessel (initial velocity $V_0 = 1$ m/s).

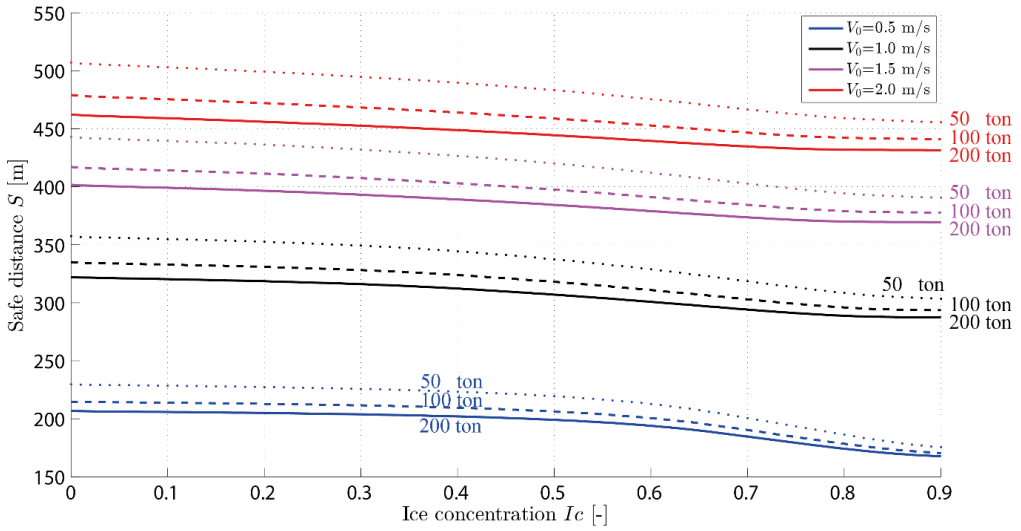

Figure 10. With a braking vessel, no collision safe distance between the GBS and towing vessels in various ice conditions with different initial velocities (note that reaction time = 10 min).

5. PROPELLER WASH AND TOWING DISTANCE

The experience with Kulluk (see Figure 1) demonstrates the effectiveness of using propeller race to facilitate rubble transportation, thereby decreasing ice resistance. The effect of propeller wash in reducing ice load has been praised by several authors (e.g., (Keinonen, 2009)). However, propeller race can also have an adverse effect by increasing the resistance (Gerwick, 2002; Nielsen, 2007). This section is devoted to studying the two conflicting effects from the towing distance.

We define two coordinate systems as in Figure 11a and b. One coordinate system (red colour x, y, z) is fixed at the considered propeller and is used to describe the velocity field behind a propeller. Another coordinate system (green colour in Figure 11b) is fixed at the centre of the

GBS and is used to position the location of the towing vessel. A typical velocity field is visualised in Figure 11b.

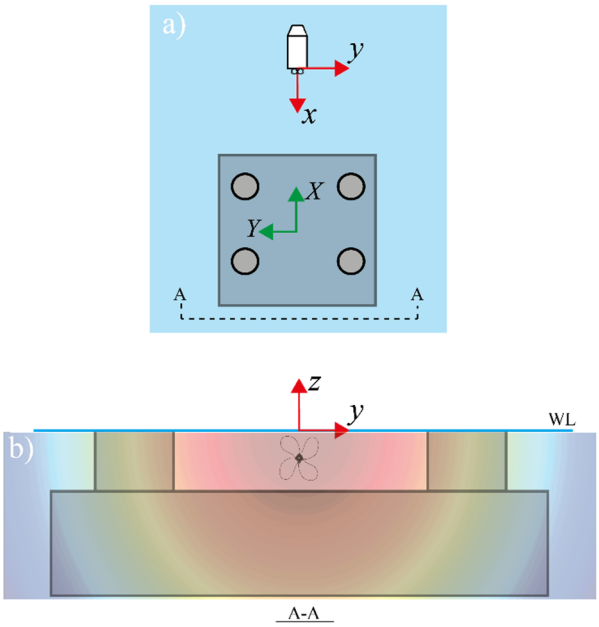

Figure 11. Coordinate systems to calculate the propeller thrust.

The normalised velocity field can be written as in Eq. (11) as documented by Nielsen (2007). The velocity is rapidly dispersed around one virtual point representing the origin of the propeller race (e.g., see the velocity distribution contour within the $x-z$ plane in Figure 12).

$$\frac{U(x,y,z)}{U_0} = \frac{1}{0.89+0.149(x/d_p)} \frac{1}{[1+\frac{0.4142((y/d_p)^2+(z/d_p)^2)}{(0.39+0.0875(x/d_p))^2}]^2} \tag{11}$$

in which,

$U(x,y,z)$ velocity distribution the virtual origin of a propeller (Nielsen, 2007);
U_0 reference velocity denoting the fluid velocity at the propeller's location;
d_p diameter of the propeller.

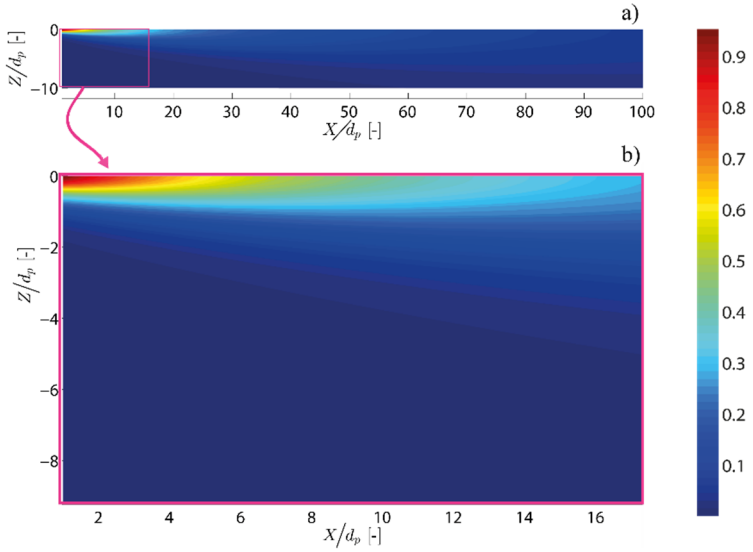

Figure 12. Velocity distribution behind a propeller.

In order to estimate how the towing distance X influences the ice clearing and resistance induced by the propeller race, it is convenient to make a primitive judgement by integrating the thrust of the fluid velocity field on the structure and hollow area, respectively. The thrust can be calculated as in Eq. (12). Considering the expression of $U(x,y,z)$ is expressed as a non-dimensional value in Eq. (11), an alternative quantification of the thruster can be expressed in Eq. (13).

$$T(x) = \frac{1}{2}\rho_w \int_A U^2(x,y,z)dA \tag{12}$$

$$T'(x) = \frac{1}{2}\rho_w \int_A \frac{U^2(x,y,z)}{U_0^2}dA \tag{13}$$

in which,

A is the integration area of specific interests. To quantify the ice clearing effect, A is illustrated in Figure 13 with blocks # 1, 2, and 3; to quantify the propeller race induced resistance, A stands for the structure's projected area within the wake (grey area in Figure 13).

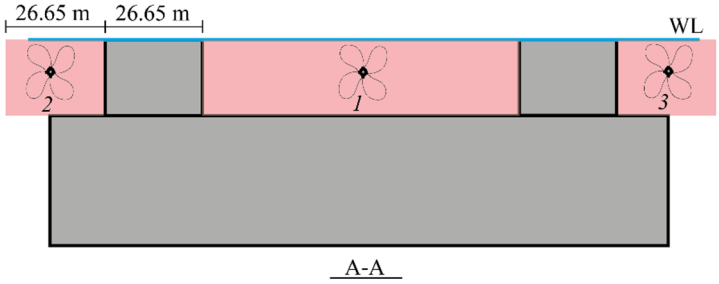

Figure 13. Thrust integration region, red: ice clearing thrust; dark: resisting thrust.

Figure 13 shows several possibilities of propeller's lateral locations (Y-direction). In the following, through a series of calculations (see the calculation matrix in Table 4), we studied the influence of propeller location. The results were plotted in Figures 14 for the case of propeller diameter $d_p = 1\,\text{m}$.

Table 4. Calculation matrix to study propeller race's effect with varying propeller's lateral location.

Example: $d_p = 1\,\text{m}$	Physical meaning
$\|Y\| = 0\,\text{m}$	propeller at the centre
$\|Y\| = 60\,\text{m}$	propeller behind the leg
$\|Y\| = 70\,\text{m}$	propeller on the side on the location of 2 or 3 as in Figure 13
$\|Y\| = 80\,\text{m}$	Same as above, but locates further side way
$\|Y\| = 90\,\text{m}$	Same as above, but locates further side way
$\|Y\| = 125\,\text{m}$	Same as above, but locates further side way
$\|Y\| = 150\,\text{m}$	Same as above, but locates further side way

The vertical axis of Figure 14 illustrate the thrust either to increase the resistance or to facilitate ice clearing effect. The horizontal axis shows that the maximum thrust resistance takes place at $X = 250\,\text{m}$; and the maximum ice clearing effect occurs at around $X = 25\,\text{m}$ for the centrally positioned propeller (i.e., $Y = 0\,\text{m}$).

The left plots of Figure 14 demonstrates that the resistance decreases if the propeller locates further sideways. On the other hand, the right plots of Figure 14 demonstrate a sudden decrease of ice clearing effect at $|Y| = 60\,\text{m}$. This shows that positioning a propeller right behind the GBS's leg tends to decrease the efficiency of ice clearing effect. Collectively, positioning a propeller

which is around $|Y| = 80$ m can both minimise the resistance and maximise the potential ice clearing effect.

For the central propeller ($Y = 0$ m), however, it appears that it is the no collision safe distance that is controlling the towing distance. The propeller race effect is not significant beyond the required no collision safe distance (see Figures 8 and 10).

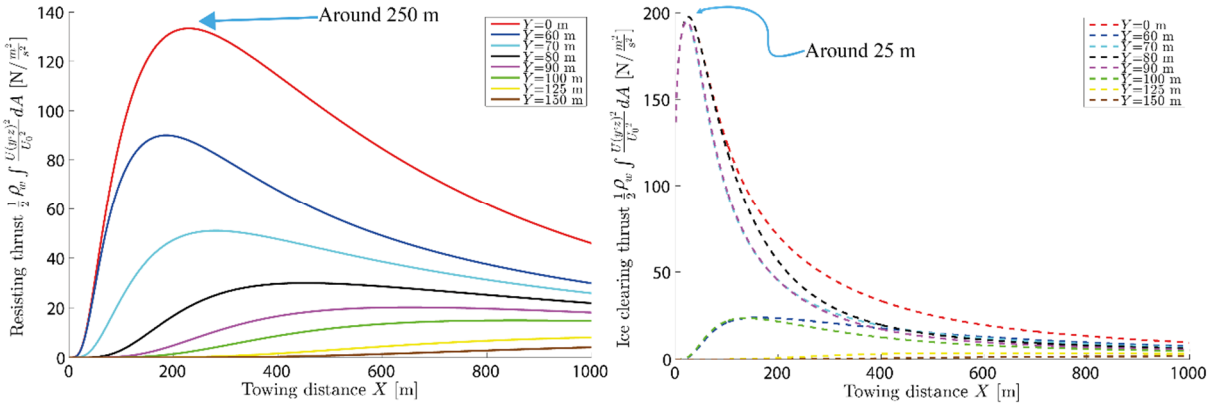

Figure 14. Resisting (left) and ice clearing (right) thrust with different towing configuration (towing distance X and lateral offset Y and $d_p = 1$ m).

6. PROPOSED TOWING CONFIGURATION AND DISCUSSIONS

After studying the upper-bound ice resistance in Section 4.1, it is found that employing 5 towing vessels with bollard pull of 200 ton each is required to tow the GBS in pressurised ice conditions. Afterwards, the no collision safe distance studied in Section 4.2 indicates that implementing a braking mechanism is beneficiary, e.g., calculations presented in Figure 10 suggest that a towing distance between 350-450 m is sufficient to cope with a towing speed of 1 m/s and 1.5 m/s respectively. Then the propeller race were studied in Section 5 to quantify the effect of towing distance for the special case with a propeller diameter of 1 m. The maximum resistance and ice clearing effect often take place while the towing distances are 250 m and 25 m respectively. For sideway positioned propellers (i.e., $|Y| > 0$), a lateral offset about 80 m can maximise the potential ice clearing effect and avoid high propeller race induced resistance.

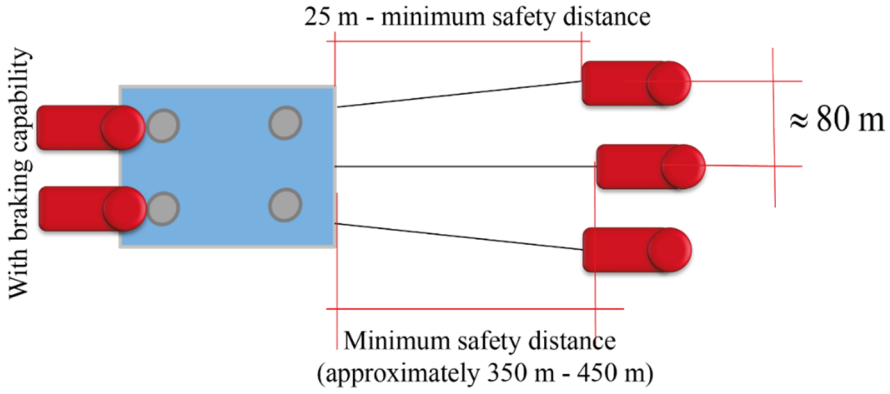

Figure 15. One of the possible options for the towing configuration.

Based on the above reasoning, a conceptual towing configuration is preliminarily proposed in Figure 15, which includes sufficient towing vessels, braking mechanism (i.e., by reversing the aft two vessels), sufficient no collision safe distance between the centrally located towing vessel and the GBS, and side vessels with maximised ice clearing effect. Particularly, the aft two vessels were partially shielded by the GBS legs, leading to less ice resistance on the aft vessels.

Similarly, Gerwick (2002) also pointed out the full efficiency of propeller's thrust could be developed with the aft vessels pushing at the rear of the structure. Furthermore, for the sake of having good manoeuvrability, the use of stern pusher vessels is recommended (Gerwick, 2002).

Several important points in designing a towing configuration have been studied in this paper. However, they are by no means exhaustive. Important topics such as the towing vessel's stability issue, motion response analysis, and more in-depth propeller wash effects should be carried out for a more rational recommendation on the towing configuration.

7. CONCLUSIONS

Towing a massive GBS in ice is challenging. This paper focuses on studying the towing configuration for the given GBS under the assumption of a reasonably managed ice environment. The major findings of the study are the following:

- In order to determine the towing configuration, an upper-bound ice resistance is estimated to first determine the number of towing vessels. The conservative calculation shows that 5 towing vessels with bollard pull 200 ton each is needed to tow the considered GBS in pressurised sea ice.
- Then a lower-bound ice resistance algorithm is proposed. The proposed model shows that there exists an ice concentration threshold, below which, rather negligible ice resistance can be encountered by the towed structure. This threshold is speed dependent (e.g., the critical ice concentration is about 55% and 75% for transiting a speed of 1 m/s and 0.5 m/s respectively). After crossing the critical ice concentration, footing failure mechanism can be utilised to estimate the lower-bound ice resistance.
- This lower bound is beneficial to estimate a no collision safe distance between the towing vessel and the GBS. Based on a series of calculations, the efficiency of reducing the no collision safe distance by a braking mechanism is quantified. Moreover, the importance of towing speed in determining the no collision safe distance is also demonstrated. For an expected towing speed in icy waters (e.g., 1 m/s and 1.5 m/s), the corresponding no collision safe distances are 350 m and 450 m with braking mechanism.
- The tow spread is further studied by investigating the effect of propeller race. For a special case with propeller diameter of 1 m, for the centrally located towing vessel, it is mainly the no collision safe distance which is controlling the towing distance. For the sideway towing vessels, it is found that a distance to the central line of 80 m can maximise the ice clearing effect and in the meantime with little collision risk. The maximum ice clearing thrust often takes place with a towing distance of 25 m.
- Based on the above findings, a towing configuration with 5 towing vessels, among which, 2 were equipped with braking mechanism are proposed. The recommended distance were also detailed.

The work presented in this paper based mainly on existing and derived analytical models. Several important aspects, but not all, for a towing configuration design were studied to achieve a preliminary conceptual design. The authors of this paper suggest that more in-depth numerical studies and model tests should be carried out as followed up studies based on the results obtained.

ACKNOWLEDGEMENT

The authors would like to thank the Norwegian Research Council through the research centre SAMCoT CRI for financial support and all the SAMCoT partners. In addition, valuable discussions with PhD students Andrei Tsarau and Marat Kashafutdinov are greatly appreciated.

APPENDIX A. DERIVATIONS OF LOWER-BOUND ICE RESISTANCE

A.1 The influencing radius

We randomly cut a square out of the considered ice field with length w as in Figure A.1a. Suppose we are able to collect all the floating ice in on corner with an area of A_i, by definite, the ice concentration can be expressed as $I_c = A_i / w^2$. Therefore, the empty space in both the horizontal and vertical direction in Figure A.1a can be written as $L_{empty} = (1-\sqrt{I_c})w$. Afterwards, we evenly distribute all the ice floes within the selected square area as in Figure A.2. Suppose that all the ice floes are of identical diameter of L_f, the amount of ice floes N in each row or column can be written as $N = \sqrt{I_c} w / L_f$. Therefore, the spacing between two adjacent ice floes can be written as $L_{space} = L_{empty} / N = (1-\sqrt{I_c})w / (\sqrt{I_c} w) \cdot L_f = (1-\sqrt{I_c}) / \sqrt{I_c} \cdot L_f$, which is independent of the selected region size. For a structure of diameter D entering into the considered ice field, we calculate how many ice floes are displaced to make room for the structure. Suppose that the structure travelled a distance of $D/2$, which is half of its diameter (see Figure 5). The number of ice floes that should be displaced are $N_{influence} = D/2 / L_{space} = \sqrt{I_c} / (1-\sqrt{I_c}) \cdot D / (2L_f)$ in either the vertical or horizontal direction. Therefore, the influencing radius is written as $R_{\text{influence}} = N_{influence} L_f = \text{Eq.(3)}$.

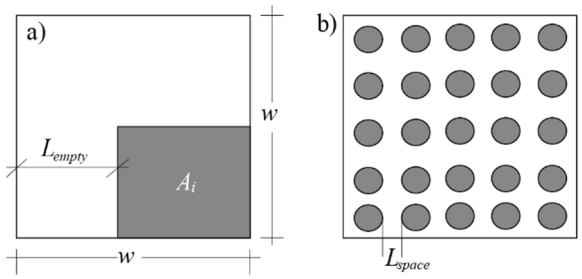

Figure A.1 Derivation plots of the influencing radius.

A.2 Derivation of Eq. (4)

Refer to Figure 5, the mass of the displaced ice floes are $m = \pi / 2[(R_{\text{influence}} + D/2)^2 - (\text{D}/2)^2]\rho_i t$. Inserting the expression of $R_{\text{influence}}$, the mass can be further written as the third term in Eq. (4). Based on the principal of momentum conservation, Eq. (4) can be derived.

REFERENCES

Browne, R., Carter, J. and Kimmerly, P., 1984. Design, Construction, and First Season's Operation of MV Kalvik and MV Terry Fox, Offshore Technology Conference. Offshore Technology Conference.

Croasdale, K.R., Bruce, J.R. and Liferov, P., 2009. Sea ice loads due to managed ice, Proceedings of the 20th International Conference on Port and Ocean Engineering under Arctic Conditions (POAC'09), Luleå, Sweden, pp. 139.

Croasdale, K.R., Comfort, G., Frederking, R., Graham, B.W. and Lewis, E.L., 1988. A pilot experiment to measure Arctic Pack-ice driving forces.

Eik, K., 2008. Review of experiences within ice and iceberg management. Journal of Navigation, 61(04): 557-572.

Faltinsen, O.M., 1993. Sea loads on ships and offshore structures, 1. Cambridge Univ Pr.

Farid, F., Scibilia, F., Lubbad, R. and Løset, S., 2014. Sea Ice Management Trials during Oden Arctic Technology Research Cruise 2013 Offshore North East Greenland, 22nd IAHR International Symposium on Ice, Singapore.

Gerwick, C., 2002. Construction of marine and offshore structures. CRC Press.

Gijzel, T., Thomson, R. and Athmer, J., 1985. Installation of the mobile arctic caisson Molikpaq, Offshore Technology Conference, Houston, Texas.

Hamilton, J., Holub, C., Blunt, J., Mitchell, D. and Kokkinis, T., 2011. Ice Management for Support of Arctic Floating Operations, OTC Arctic Technology Conference.

Hnatiuk, J. and Wright, B., 1984. Ice management to support the Kulluk drilling vessel, Annual Technical Meeting. Petroleum Society of Canada.

Keinonen, A., 2009. Innovative Ice Management Icebreaker, Proceedings of the 20th International Conference on Port and Ocean Engineering under Arctic Conditions, Luleå, Sweden, pp. 138.

Loh, J., Stamberg, J. and Cusack, K., 1984. New Generation Arctic Drilling System: Overview of First Year's Performance.

Lu, W., 2014. Floe Ice - Sloping Structure Interactions. Doctoral Thesis, Norwegian University of Science and Technology, Trondheim.

Lu, W., Lubbad, R. and Løset, S., 2015a. In-plane fracture of an ice floe: A theoretical study on the splitting failure mode. Cold Regions Science and Technology, 110(0): 77-101.

Lu, W., Lubbad, R. and Løset, S., 2015b. Out-of-plane failure of an ice floe: radial-crack-initiation-controlled fracture. Cold Regions Science and Technology.

Lu, W., Lubbad, R., Løset, S. and Kashafutdinov, M., 2015c. Fracture of an ice floe: Local out-of-plane flexural failures versus global in-plane splitting failure. Cold Regions Science and Technology.

Lubbad, R. and Løset, S., 2011. A numerical model for real-time simulation of ship-ice interaction. Cold Regions Science and Technology, 65(2): 111-127.

Maddock, B., Bush, A., Wojahn, T., Kokkinis, T., Younan, A. and Hawkins, J.R., 2011. Advances in ice management for deepwater drilling in the Beaufort Sea, Proceedings of the International Conference on Port and Ocean Engineering Under Arctic Conditions.

Marchenko, A., Kulyakhtin, A. and Eik, K., 2010. Icebergs drift in the Barents Sea: data analysis of ice tracking buoy and numerical simulations, 20th IAHR International Symposium on Ice, Lahti, Finland.

Metrikin, I. and Løset, S., 2013. Non-Smooth 3D Discrete Element Simulation of a Drillship in Discontinuous Ice, Proceedings of the 22nd International Conference on Port and Ocean Engineering under Arctic Conditions, Espoo, Finland.

Nielsen, F.G., 2007. Lecture notes in marine operations. Department of Marine Structures, Norwegian University of Science and Technology, Trondheim, Norway.

Palmer, A.C. and Croasdale, K.R., 2013. Arctic Offshore Engineering. World Scientific.

Scibilia, F., Metrikin, I., Gürtner, A. and Teigen, S.H., 2014. Full-scale trials and numerical modeling of sea ice management in the greenland sea, OTC Arctic Technology Conference. Offshore Technology Conference.

Tsarau, A., Lubbad, R. and Løset, S., 2015. Recent advances in modelling the hydrodyanmic effects on ice motion and ice-structure interactions offshore, The 23nd International Conference on Port and Ocean Engineering under Arctic Conditions, Trondheim, Norway.

Tsarau, A., Løset, S. and Grindstad, T., 2014. Propeller wash by an icebreaker, 22nd IAHR International Symposium on Ice Singapore.

Veritas, D.N., 2011. Modelling and analysis of marine operations. Oslo, Norway.

Walsh, M., Drolet, J. and Eddy, P., 1994. Movement And Placement Of Large Offshore Drilling Structures In The Arctic, Offshore Technology Conference. Offshore Technology Conference.

Wright, B., 1998. Moored Vessel Stationkeeping in Grand Banks Pack Ice Conditions.

Wright, B., 1999. Evaluation of full scale data for moored vessel stationkeeping in pack ice. PERD/CHC Report: 26-200.